ChemSusChem

Research Article
doi.org/10.1002/cssc.202201505

Chemistry Europe
European Chemical Societies Publishing

www.chemsuschem.org

Incorporation of Conjugated Diynes in Perovskites and their Post-Synthetic Modification

Priscila I. Román-Román,[a] Carmen Ortiz-Cervantes,[b] Jessica I. Vasquez-Matias,[a] Josué Vazquez-Chavez,[b] Marcos Hernández-Rodríguez,[b] and Diego Solis-Ibarra*[a]

Two-dimensional (2D) organic–inorganic hybrid perovskites have rapidly become an attractive alternative to three-dimensional (3D) perovskites as solar cell absorbers, owing to their improved stability, versatility, and ease of processing. Despite their advantages, the insulating nature of the organic cations makes these materials have lower absorbing and conducting properties, resulting in lower device efficiencies. A way to circumvent these issues is the integration of functional molecules that help mitigate these limitations. In this study, six new perovskites composed of three distinct diynes are synthesized, all of which can be thermally polymerized to form conjugated polymers within the perovskite layers. The incorporation of conjugated polymers results in drastic changes in these materials' optoelectronic properties and their overall stability. Furthermore, depending on the nature of the diyne and the inorganic layers, the materials show varying polymerization yields, optical bandgaps, and charge carrier densities. These results afford significant insight into the chemical nature of the polymerized species and thus highlight the versatility of this approach to post-synthetically generate conducting polymers within the layers of 2D perovskites, paving the way toward their use in optoelectronic devices.

Introduction

Two-dimensional (2D) halide perovskites described by the formula $(A')_2M^{2+}X_4$ have arisen as a new platform due to their promising optoelectronic applications, such as in photovoltaics (PV), light-emitting diodes (LEDs), photodetectors and others.[1,2] Among other advantages, 2D perovskites have demonstrated to enhance the stability of perovskite solar cells, thanks to the hydrophobic organic cations that hinder moisture damage.[3] However, the insulating nature of the organic cations results in reduced absorption and conductivity, leading to a decrease in power conversion efficiency (PCE).[4] To date, most organic cations contained into 2D perovskites show unfavorable properties such as large energy band gap, high exciton binding energy, and low charge carrier transport.[5,6] Nevertheless, introducing tailored organic spacers can tune the overall electronic properties to overcome these issues for targeted optoelectronic applications. In this regard, some approaches using π-conjugated moieties such as oligothiophene and aromatic pyrene have achieved enhanced optoelectronic properties.[7–9] For example, bulky and hydrophobic cations based on tetrathiophene backbone were used to furnish single-crystalline 2D perovskites; such ligands were able to modulate crystal morphology and electronic properties with improved materials stability.[10] Using conjugated moieties with the form (pyrene-O-linker-NH_3), photovoltaic properties–out-of-plane conductivity and band gap–were improved.[8] Recently, we reported that insertion of deca-3,5-diyn-1-ammonium (henceforth DDA) and subsequent thermal treatment resulted in the topochemical polymerization of the diyne to yield a highly crystalline hybrid perovskite that contains a conducting polymer in its structure. Interspersing this polymer into the perovskite structure resulted in a 1.6 eV shrinkage of the bandgap and an increase in electric conductivity of up to three orders of magnitude.[11] Despite this exciting result,[12] to date, there is only one perovskite material ($[DDA]_2PbBr_4$) for which this thermo-polymerization approach has proven to work.

Moreover, little to nothing has been reported regarding the polymerization process efficiency or effects on the material's macroscopic properties. In this manuscript, we studied the incorporation of several diynes and the effect of changing the halide from bromide to chloride or iodide has in the polymerization process and, ultimately, on the optical and hydrophobic properties of these materials (Figure 1). Our results highlight this approach's versatility towards improving the properties of hybrid perovskites, showing that it applies to diverse inorganic layers and varied organic diynes. Also, it paves the way for further improvements in the area; mainly, it shows that upgrading the polymerization efficiency could have even more drastic effects on the absorption, conductivity, and stability of these materials, leading to make better materials and devices.

[a] P. I. Román-Román, J. I. Vasquez-Matias, Prof. D. Solis-Ibarra
Instituto de Investigaciones en Materiales
Universidad Nacional Autónoma de México (UNAM)
Circuito Exterior S/N, Coyoacán, CDMX 04510 (Mexico)
E-mail: diego.solis@unam.mx

[b] Prof. C. Ortiz-Cervantes, Dr. J. Vazquez-Chavez, Prof. M. Hernández-Rodríguez
Instituto Química, Universidad Nacional Autónoma de México (UNAM)
Circuito Exterior S/N, Coyoacán, CDMX 04510 (Mexico)

Supporting information for this article is available on the WWW under https://doi.org/10.1002/cssc.202201505

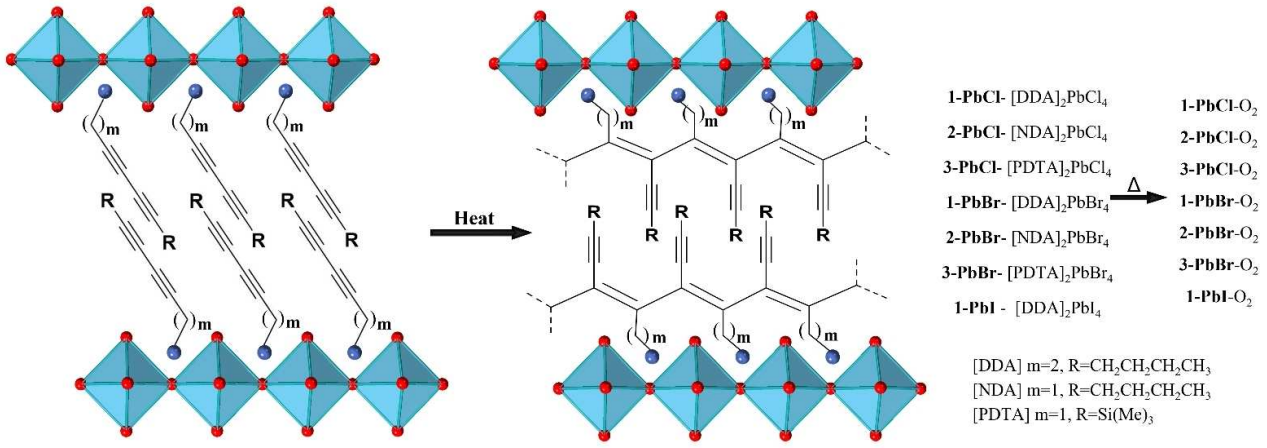

Figure 1. Schematic representation of the heat-induced polymerization within 2D halide perovskites.

Results and Discussion

Previously, we demonstrated that $[DDA]_2PbBr_4$ (**1-PbBr**) drastically improves its properties upon heating.[11] However, during the topochemical polymerization, the diynes polymerize in a stochastic manner[12] that could lead to distinct polymeric species, varied properties, and hence, a widely diverse set of materials and possible applications. If that hypothesis is true, small changes in the structure could lead to different products and several properties. For instance, one would expect the halide present in the lead perovskite to have a strongly influence on the polymerized product properties, as those would have a direct impact in intermolecular interactions and distances.[1] Furthermore, we wanted to prove if it is possible to extend this approach to other diynes and halide perovskites. To do so, we decided to synthesize three distinct cations and try to include them into lead chloride, bromide, and iodide perovskites. Besides proving how broadly applicable this phenomenon is, this would also allow us further to understand the polymerization process and its impact on the materials' properties.

The synthesis of ligands and perovskites with different halides was based on our previously reported method.[11] For the synthesis of conjugated dialkynyl ammonium chlorides, we obtained 2,4-nonadiyn-1-ammonium (**2** or NDA) chloride or and 2,4-pentadiyn-5-trimethyl silyl-1-ammonium (**3** or PDTA) chloride from commercially available precursors in only two synthetic steps with good yields (see the Supporting Information for synthetic details). Using these two new ligands (NDA and PDTA) and the previously reported (DDA or **1**), six new lead halide perovskites, namely $[DDA]_2PbCl_4$ (**1-PbCl**), $[DDA]_2PbI_4$ (**1-PbI**), $[NDA]_2PbCl_4$ (**2-PbCl**), $[NDA]_2PbBr_4$ (**2-PbBr**), $[PDTA]_2PbCl_4$ (**3-PbCl**), and $[PDTA]_2PbBr_4$ (**3-PbBr**), were successfully obtained as a polycrystalline powders in good yields by changing halogen from bromide to chloride and iodide (see the Supporting Information for synthetic details). All these materials were thoroughly characterized, and all showed to have a 2D halide perovskite structure. Unfortunately, we were unable to obtained lead iodide perovskites with NDA and PDTA, likely due to solubilities discrepancies with the PbI_2.

Inspired by our previous work,[11] we then studied thermal behavior of the obtained materials. By using thermogravimetric analysis (TGA) we found that **1-PbCl**, **1-PbBr**, **1-PbI** and **3-PbBr** were thermally stable up to 393 K while decomposition temperatures for **2-PbCl**, **2-PbBr** and **3-PbCl** were all above 433 K. Therefore, each material was heated under air at 393, 403 or 433 K to obtain the, presumably polymerized, oxygen-doped (-$\mathbf{O_2}$) 2D perovskites structures (see the Supporting Information for further details). Remarkably, all these materials showed a color change upon heat treatment, and most of these showed dramatic color changes. In contrast to our expectations, the minimum transition temperature for the materials was not significantly altered, and only a discrete variation was observed (393–433 K). The latter is significant considering their potential use in methylammonium containing, Ruddlesden–Popper perovskites, as the transition temperatures are well beyond methylammonium evaporation temperatures.

The drastic change in colors prompted us to study the resulting materials further. First, we looked at the powder X-ray diffraction (PXRD), which showed that the materials retain high crystallinity with preferential growth along the $<100>$ plane upon heat treatment, regardless of the organic ligand or halide used (Figure 2). Therefore, it is possible to confirm that these materials preserve their 2D perovskite structure after heat-induced polymerization. Noteworthy is that, unlike our previous work, not all of these materials show significant unit cell expansion. Other than **1-PbBr** and **1-PbI**, all others showed discrete changes in unit cell size (Figures 2 and S9). The differences in unit cell sizes are likely associated with packing of the organics in the non-treated materials and how much stress the polymerization process induces in the overall material.

The preferential orientation and high crystallinity that these compounds possess mostly allow us to observe the inorganic part of the material, so a different technique such as vibrational spectroscopy is necessary to analyze the organic part. Interestingly, when we analyzed the IR spectra of the materials before

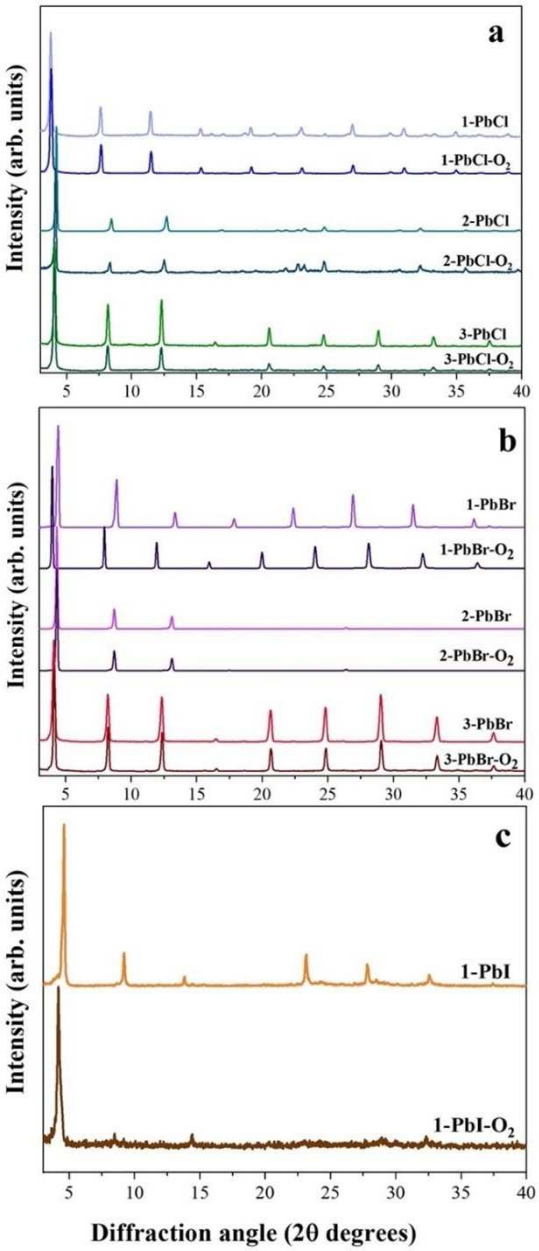

Figure 2. Powder X-ray diffraction (PXRD) patterns before and after heat treatment at 393 K to 433 K for 24 h. a) chloride perovskites, b) bromide perovskites and c) iodine perovskite.

and after polymerization, new bands were detected, particularly a wide one at 1600–1700 cm^{-1} (Figure S10), which is consistent with the formation of polyacetylene molecules.[13] Also, in the IR spectra of the heat treated materials is possible to identify non-polymerized DDA, NDA, of PDTA, which, confirms that the polymerization process does not occur in a quantitative manner. Thus, to estimate the polymerization yield, we performed quantitative nuclear magnetic resonance (qNMR) analysis to quantify the amount of unpolymerized monomers,[14] and consequently, the amount of polymerized material (Table 1). From these results, it is clear that polymerization efficiency depends on the specific cation and halide, with yields

Table 1. Summary of polymer characterization.

Material	Polymerization yield [%][a]	M_w [g mol^{-1}][b]	M_w/M_n[c]	Spins [mol^{-1}][d]
1-PbCl-O_2	36.1	1199	2.82	4.90E+18
2-PbCl-O_2	79.1	979	2.34	1.8E+19
3-PbCl-O_2	N.D[f]	1619	2.68	3.80E+19
1-PbBr-O_2[e]	85.3	139360	1.92	2.35E+19
		1066	2.93	
2-PbBr-O_2	64.6	2915	2.31	4.70E+20
3-PbBr-O_2	N.D[f]	3353	4.56	1.90E+20
1-PbI-O_2	77.7	1829	2.97	6.80E+19

[a] Polymerization yield determine by quantitative NMR of the digested samples. [b] M_w is average molecular weight. [c] M_w/M_n is polydispersity index (PDI). [d] As determined by quantitative solid-state EPR measurements. [e] Two polymeric species were found for this. The relative abundance for these fragments where 79.8 and % 20.2 for the high and low M_w fragments respectively. [f] N.D = not determined.

that range from 36 to 85%. Also, to better understand the chemical nature of the obtained materials, we carried ^{13}C NMR analysis on the polymerized material **1-PbBr-O_2** (Figure S21). This analysis showed the presence of new *sp* and sp^2 carbons, which is consistent with a polymeric structure such as that depicted in Figure 1, and is also consistent with previous reports.[11,12]

We then characterized the color change by UV/Vis—NIR absorption spectroscopy of the materials before and after thermal treatment. Before heat treatment, the materials displayed absorption behavior typical of the respective 2D halide perovskite family. For example, lead chloride perovskites (**1-PbCl**, **2-PbCl** and **3-PbCl**) showed bandgaps of around 3.8 eV, whereas their lead bromide (**1-PbBr**, **2-PbBr** and **3-PbBr**) and iodide (**1-PbI**) analogs showed bandgaps of around 3.0 eV and 2.4 eV respectively. After thermal treatment, most of these materials' absorption spectra changed drastically, with many of them showing absorption well into the near IR (NIR) region of the spectra (Figure 3). The materials synthesized from lead bromide (**1-PbBr**, **2-PbBr**, and **3-PbBr**) and lead iodide (**1-PbI**) behave similarly and all showed a significant change in bandgap, with the maximum reduction of 1.8 eV for **1-PbBr-O_2**. The absorption data of **1-PbBr-O_2** and **3-PbBr-O_2** shows a new shoulder at approximately 500 nm; which is consistent with the topochemical formation of polydiacetylene residues.[15, 17] Notably, the absorption of **1-PbI- O_2** is very similar to that of **1-PbBr-O_2** (Figure 3c), which suggests that similar polymeric species are being formed, which in turn dictates the absorption of these materials. Also, the bandgap for these materials (**1-PbBr-O_2** and **1-PbI-O_2**) is approximately 1.5 eV, which makes them suitable candidates for application as single-junction solar cells absorbers.[16] In contrast, for lead chloride materials (**1-PbCl**, **2-PbCl**, and **3-PbCl**), the change in absorption is not as drastic, with maximum bandgap reduction of 0.8 eV for **2-PbCl**, and an almost negligible change for **1-PbCl**.

To gain a better insight into the nature of the obtained polymer and the overall polymerization process, we performed gel permeation chromatography/high-performance size exclusion chromatography (GPC/HPSEC). The results obtained indicate that the topochemical polymerization produces materials

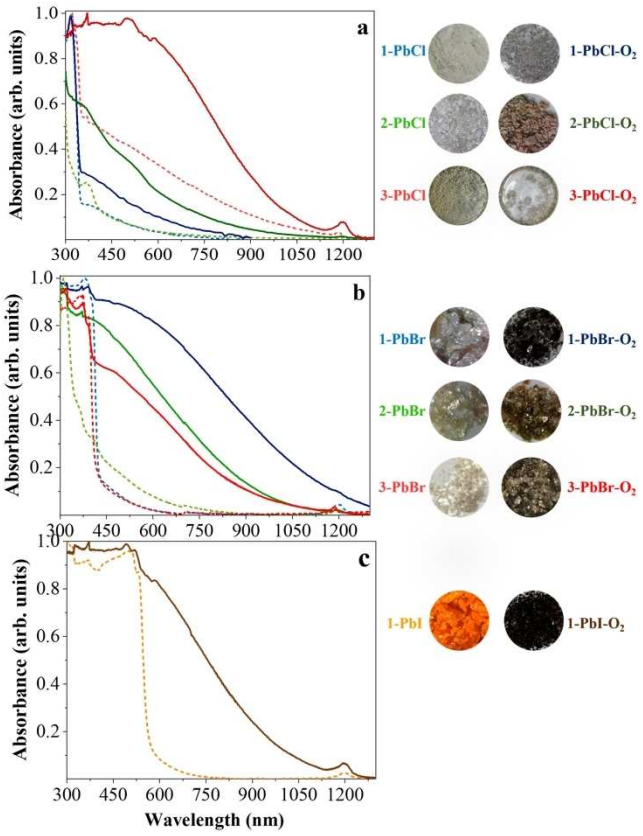

Figure 3. Absorption of chloride, bromide, and iodide perovskites: a) DDA (**1Cl**, **1Cl-O$_2$**), NDA (**2Cl**, **2Cl-O$_2$**) and PDTA (**3Cl**, **3Cl-O$_2$**); b) DDA (**1Br**, **1Br-O$_2$**), NDA (**2Br**, **2Br-O$_2$**) and PDTA (**3Br**, **3Br-O$_2$**); c) DDA (**1I**, **1I-O$_2$**) with no treatment and heat treatment at 393 K to 433 K for 24 h.

with diverse characteristics depending on the monomer and the metal-halide layer. The material with the largest formed polymer is **1-PbBr-O$_2$**, which presented an average molecular weight (M_w) of 139360 g mol^{-1} and a polydispersity index (PDI) of 1.92. The GPC/HPSEC results also suggest that lead chloride perovskites tend generate smaller polymers compared with the bromide and iodide perovskites. This could be because lead chloride perovskites provide a more constrained environment for the diyne molecules, which in turns, hamper the movement needed for an efficient polymerization. The reason for this is two-fold, first, the shorter Pb–Cl bonds generate molecules that are more closely packed. Secondly, the N–H···Cl hydrogen bonds are stronger than the corresponding hydrogen bonds in bromide or iodide materials, which also restrict diyne movement. From these results, it can also be noted, that **1-PbBr-O$_2$** forms chains that are up to around 900 units long, whereas the other materials presented only produce short-chain oligomers (7–22 units long). The latter compares well with the report from Sanui and co-workers, which found that gamma-ray irradiation of diyne-perovskites can form polymers of 22–27 units.[15]

During our GPC/HPSEC studies, we were not able to find a direct relationship between polymer size and bandgap of the material. We then hypothesize that the light absorption of these materials depends not only in the polymer size, but also in the polymerization yield, and in the amount of polymer doping. In fact, it has been demonstrated that the oxygen in the air during heat treatment generates free radicals that are in turn responsible for the enhanced absorption and electronic conductivity.[11] Thus, using electronic paramagnetic resonance (EPR) we quantified the amount of charge carriers in these materials (Table 1). The lowest concentration of spins is observed in the chloride-based materials, and the highest in **2-PbBr-O$_2$**. The fact that the smaller spin densities are found in the chloride materials is likely associated to the fact that, as discussed earlier, chloride-based perovskites tend to form the smallest polyacetylenes and, have lower polymerization yields. Importantly, the doping levels obtained herein, were obtained "naturally", while heat treating the materials under air. However, an interesting research avenue will be to explore other doping strategies, such as the use more oxidant atmospheres.

Another potential advantage of inserting polymer into perovskites is to improve their hydrophobicity and consequently, their stability towards humidity and water in general. Thus, we studied the contact angle of films made of the materials before and after heat treatment (Figures 4 and S13). Notably, the hydrophobicity of the materials increases after heat treatment. This change is dependent on the halide that forms the perovskite (Cl, Br, or I). As shown in Figure 4, chloride perovskites show a slight change, while iodide perovskite present a drastic increase. Again, this could be attributed to the more limited polymerization of the chloride-based perovskites. Beyond hydrophobicity, we also conducted stability studies of DDA-based materials (1-PbX and 1-PbX-O$_2$, where X = Cl, Br, and I) upon exposure to humid conditions (ca. 23 °C and 60% relative humidity, Figure S24). These studies revealed that in all three cases, the heat-treated samples (**1-PbX-O$_2$**) are more stable under these conditions than their non-treated (**1-PbX**) counterparts. Thus, by combining contact angle and stability

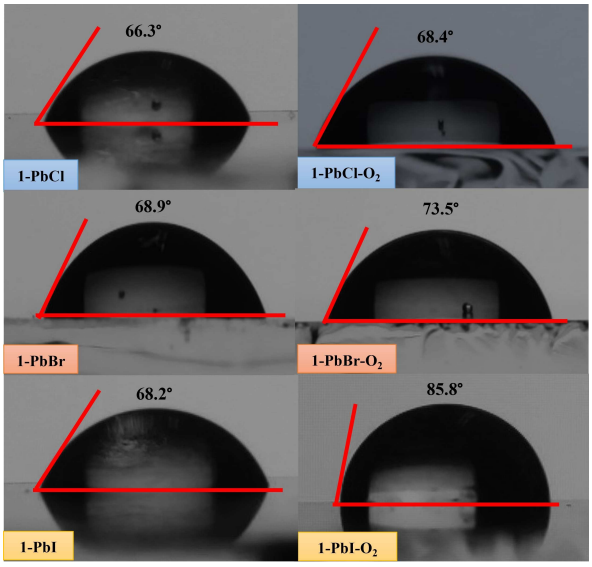

Figure 4. Contact angle measurements before and after heat treatment at 393 K to 433 K for 24 h. for DDA perovskites (**1-PbCl**, **1-PbBr** and **1-PbI**).

measurements, we can corroborate that the polymerization process improves the overall stability towards humidity of the material. On the other hand, the thermal stability of the materials is not significantly altered, as can be observed in their corresponding thermogravimetric and calorimetric analyses (Figures S14–S16).

Conclusions

We have demonstrated that multiple diyne-containing perovskites undergo a thermal polymerization process to form 2D perovskites with polydiacetylenes within their inorganic layers. In doing so, we proved that using diynes is a robust strategy applicable to various diynes and halides. By expanding the library of possible diynes and halides, as well as the characterization techniques used, we have better understood the polymerization process and how it affects the properties of the resulting materials. In general, we observed that all the materials studied underwent heat-induced polymerization to various extents, which resulted in substantial changes to their optoelectronic properties. Also, by studying the generated polymers, we confirmed the structure of the generated polyacetylenes and observed that the formation process varies widely in terms of polymerization yield, polymer size, polydispersity, and spin density. The combination of all these factors ultimately determines the properties of the final materials. Currently, it is impossible to provide comprehensive guidelines on how the inorganic layer type or diyne structure affects the final polymer properties. However, we have noted that chloride perovskites (**1-PbCl**, **2-PbCl**, and **3-PbCl**) tend to generate smaller polymers with lower spin concentrations than their bromide and iodide analogs. Furthermore, beyond the improvement in optoelectronic properties, we demonstrated that introducing polydiacetylenes into 2D hybrid perovskites can significantly enhance the materials' hydrophobicity and stability towards humidity.

Unfortunately, to date, all diyne-containing perovskites require high polymerization temperatures, making this approach incompatible with Ruddlesden–Popper or Dion–Jacobson perovskites, particularly those that incorporate methylammonium. Consequently, future efforts should be devoted to lowering the polymerization temperature and improving the polymerization yield, both of which will likely result in larger, less polydisperse polymers and, ultimately, in better materials able to function as capable absorbers for solar cells.

Experimental Section

General considerations

All reagents were purchased from commercial sources and used as received: 1-hexyne (97%), *N*-(3-butynyl) phthalimide (97%), *N*-Boc-propargylamine (97%), *N*,*N*,*N*',*N*'-tetramethylethylenediamine (TMEDA, 99%), hydrazine hydrate (50–60%), copper(I) iodide (CuI, 98%), lead(II) iodide (PbI_2, 99%), lead(II) bromide ($PbBr_2$, 98%), lead(II) chloride ($PbCl_2$, 98%), hydroiodic acid (HI, 57 wt% in H_2O), copper (II) acetate monohydrate (98%), ethynyltrimethylsilane (98%), pyridine anhydrous (99.8%), tetrahydrofuran anhydrous (THF, 99%), hydrobromic acid (HBr, 48%), hydrogen chloride solution 4.0 M in dioxane. Solvents were of reagent grade o higher purity. 3,5-decadiyn-1-ammonium chloride (DDA·Cl) was synthetized according to the reference.[11] All manipulations were conducted in air unless otherwise specified. Ethyl ether, methanol, toluene, DMF and acetonitrile were dried and degassed using a JC Meyer solvent purification system.

Synthesis of organic ligands and perovskite materials

Detailed synthetic and characterization of DDA chloride, NDA chloride, PDTA chloride; and the corresponding perovskites: $[DDA]_2PbCl_4$ (**1-PbCl**), $[DDA]_2PbI_4$ (**1-PbI**), $[NDA]_2PbCl_4$ (**2-PbCl**), $[NDA]_2PbBr_4$ (**2-PbBr**), $[PDTA]_2PbCl_4$ (**3-PbCl**), and $[PDTA]_2PbBr_4$ (**3-PbBr**), can be found in the Supporting Information.

Heat-induced polymerization

Samples were placed on 3 mL glass ampoules and sealed under air atmosphere (O_2). The sealed ampoules were heated for 24 h in a range of 393 K to 433 K, depending on the material. Details on the conditions can be found in Table S2. The typical samples sizes varied from 50 mg to 100 mg. When the heating time was over, the samples were allowed to cool to room temperature.

Characterization methods

NMR spectroscopy

NMR solution spectroscopy was done in a spectrometer Bruker Avance III HD 400 MHz with a probe BBI 400 MHz SB 5 mm with z-gradient. The frequencies were 400.17 MHz for ^1H and 100.63 MHz for ^{13}C. The samples were dissolved in chloroform ($CDCl_3$) Sigma Aldrich CAS 865-49-6 and/or dimethyl sulfoxide (DMSO-d_6) Sigma Aldrich CAS 2206-27-1, filtered and placed in standard NMR tube.

Mass spectrometry

A Jeol mass spectrometer SX 102 A was used with the direct analysis in real time (DART) technique using acetone or methanol as solvents. LCQTOF ESI MS 6200 series TOF/6500 series (HPLC-EM-SQ-TOF Agilent Tech G6530BA.

Optical characterization

Absorption measurements were recorded using a Shimadzu spectrophotometer (UV-2600) equipped with an integrated sphere and collected using absorbance data on a bulk powder sample.

Powder X-ray diffraction (PXRD)

Powder X-Ray diffraction measurements were performed on a Rigaku Ultima IV diffractometer with $Cu_{K\alpha}$ radiation ($\lambda = 1.54056$ Å) at 40 kV and 44 mA. The instrument was operating in a Bragg Brentano geometry with a step increment of 0.02° and an acquisition time of one second per step.

FTIR spectroscopy

A Bruker FTIR ALPHA spectrometer with a total attenuated reflection module (ATR) was used, measuring 32 scans per sample, from 4000 to 400 cm^{-1} with a resolution of 2 cm^{-1}, the sample did not require previous preparation.

Polymerization yield by qNMR

To calculate the polymerization yield, we used an adaptation of the method reported by Pareja-Rivera et al.[14] The standard certified used for this experiment was TCNB (1,2,4,5-Tetrachloro-3-nitrobenzene, TraceCERT, Sigma Aldrich). Briefly, using an analytical balance we weighted the synthesized perovskites (ca. 10 mg) after the thermal treatment and sonicated them for 30 min in 0.6 mL of DMSO-d_6. The resulting solution was filtered, placed in an NMR-tube with a known amount of internal standard (ca. 10 mg) and homogenized with a vortex. Then, an ^{1}H NMR spectrum was measured, using 32 scans and an extra-long t_1 time of 1 s to ensure accurate quantification. The resulting NMR spectra was then integrated and the signals from the non-labile carbon-bound protons were normalized to the signal from the internal standard. As the integrated peak of each signal is directly proportional to the number of protons, these results allowed us to determine the absolute mass of the remaining non-polymerized organic ligand, and by thus, the polymerization yield.

Electron paramagnetic resonance (EPR) spectroscopy

Solid samples were placed in quartz tubes of 1.34 cm in diameter and thickness of.0.15 cm. Loaded tubes were then introduced in a Jeol JES-TE300 spectrometer operating at X band frequency (9.4 GHz) at 100 kHz field modulation, with a cylindrical cavity (TE011 mode). Samples were run at 77 K except for spin quantifications, which were performed at room temperature using 1/C as pitch.

Gel permeation chromatography/high-performance size exclusion chromatography

GPC/HPSEC analyzers were equipped with UV/Vis detector. The molecular weights and the molecular distributions (MWD) of the samples from perovskite digestion were determined by GPC chromatography in Water Alliance e2695 chromatograph separation module apparatus equipped with detector multi-angle light-scattering (MALLS) Wyatt Technology, model DAWN EOS, polystyrene was used for calibration. The samples were dissolved in THF.

Angle contact measurements

To examine hydrophobicity of the materials, water contact angles were gained using a contact angle goniometer (L2004 A1, Ossila). For this purpose, thin films were fabricated via spin-coating the DMF precursor solutions of perovskite on PEDOT:PSS substrates. Glass substrates (2.5 cm × 2.5 cm) were cleaned by sonication in detergent, water, ethanol, acetone, isopropanol and dried with nitrogen flow before use. A PEDOT:PSS layer was deposited onto the substrates by spin coating at 2000 rpm for 1 min using a commercial PEDOT:PSS solution. The substrates were then annealed by heating at 373 K for 30 min. The perovskite layers were deposited by spin-coating 0.2 M Pb^{2+} perovskite precursor solutions at 1500 rpm for 1 min. The 0.2 M Pb^{2+} precursor solutions of were prepared by dissolving the corresponding amount of perovskite powders in anhydrous dimethylformamide (DMF).

Thermogravimetric analysis (TGA) and differential scanning calorimetry (DSC)

Thermogravimetric analysis was performed in a TGA Q5000 V3.17 Build 265 (TA Instruments) under nitrogen atmosphere (flow rate 10 mL min^{-1}) with a platinum pan at a heating rate of 5 °C min^{-1}. A room temperature (RT) to 500 °C range was used. Differential thermal analysis was performed with a DSC Q2000 V24.11, Built 124 (TA instruments) under nitrogen atmosphere (flow rate 50 mL min^{-1}) with aluminum pan at a heating rate of 5 °C min^{-1}. RT to 250 °C range was used. Discontinuities at 45.9 °C and 172.8 °C are present in the differential thermal analysis in the 4 samples, this is due to the start/end of heating and cooling cycles.

The equipment SDT Q600 V8.3 Build 101 (Simultaneous DSC/TGA) provides a simultaneous measurement of weight change (TGA) and differential heat flow (DSC) on the same sample from RT to 500 °C. This sample was heated from 25 to 600 °C, with a heating ramp of 5 °C min^{-1} under air atmosphere.[17]

Acknowledgements

We acknowledge the financial support from PAPIIT IN216020 and CONACYT's CB-A1-S-8729. We are grateful to Prof. Hao Yan for valuable discussions and to Prof. A. Paulina Gómora-Figueroa for granting us access to several instruments. Finally, we acknowledge the support from Virginia Gómez-Vidales, Salvador López, Adriana Tejeda, Gerardo Cedillo, Carlos Ramos, Eriseth Morales, Ana Bobadilla, Alejandro Pompa, Cain González, and Miguel Angel Canseco.

Conflict of Interest

The authors declare no conflict of interest.

Data Availability Statement

The data that support the findings of this study are available from the corresponding author upon reasonable request.

Keywords: 2D materials · perovskites · polymers · solar cells · topochemistry

[1] C. Ortiz-Cervantes, P. Carmona-Monroy, D. Solis-Ibarra, *ChemSusChem* **2019**, *12*, 1560–1575.
[2] L. Mao, P. Guo, M. Kepenekian, I. Spanopoulos, Y. He, C. Katan, J. Even, R. D. Schaller, R. Seshadri, C. C. Stoumpos, M. G. Kanatzidis, *J. Am. Chem. Soc.* **2020**, *142*, 8342–8351.
[3] I. C. Smith, E. T. Hoke, D. Solis-Ibarra, M. D. McGehee, H. I. Karunadasa, *Angew. Chem. Int. Ed.* **2014**, *53*, 11232–11235; *Angew. Chem.* **2014**, *126*, 11414–11417.
[4] B. Sun, Y. Xu, Y. Chen, W. Huang, *APL Mater.* **2020**, *8*, 040901.
[5] K. Zheng, T. Pullerits, *J. Phys. Chem. Lett.* **2019**, *10*, 5881–5885.
[6] J. Hu, L. Yan, W. You, *Adv. Mater.* **2018**, *1802041*, 1–10.
[7] D. B. Mitzi, C. A. Feild, W. T. A. Harrison, A. M. Guloy, *Nature* **1994**, *369*, 467–469.
[8] J. V. Passarelli, D. J. Fairfield, N. A. Sather, M. P. Hendricks, H. Sai, C. L. Stern, S. I. Stupp, *J. Am. Chem. Soc.* **2018**, *140*, 7313–7323.

[9] X. Zhu, N. Mercier, P. Fre, P. Blanchard, J. Roncali, M. Allain, C. Pasquier, *Inorg. Chem.* **2003**, *42*, 2–4.
[10] Y. Gao, E. Shi, S. Deng, S. B. Shiring, J. M. Snaider, C. Liang, B. Yuan, R. Song, S. Janke, A. Liebman-Peláez, P. Yoo, M. Zeller, B. W. Boudouris, P. Liao, C. Zhu, V. Blum, Y. Yu, B. M. Savoie, L. Huang, L. Dou, *Nat. Chem.* **2019**, *11*, 151–115.
[11] C. Ortiz-Cervantes, P. I. Román-Román, J. Vazquez-Chavez, M. Hernández-Rodríguez, D. Solis-Ibarra, *Angew. Chem. Int. Ed.* **2018**, *57*, 13882–13886; *Angew. Chem.* **2018**, *130*, 14078–14082.
[12] Y. Takeoka, K. Asai, M. Rikukawa, K. Sanui, *Chem. Commun.* **2001**, *1*, 2592–2593.
[13] R. Rodriguez-abad, J. Tsibouklis, *Synth. Commun.* **1998**, *28*, 4333–4338.
[14] C. Pareja-Rivera, A. L. Solís-Cambero, M. Sánchez-Torres, E. Lima, D. Solis-Ibarra, *ACS Energy Lett.* **2018**, *3*, 2366–2367.
[15] W. L. Xu, M. D. Smith, J. A. Krause, A. B. Greytak, S. Ma, C. M. Read, L. S. Shimizu, *Cryst. Growth Des.* **2014**, *14*, 993–1002.
[16] J. Yan, W. Fu, X. Zhang, J. Chen, W. Yang, W. Qiu, G. Wu, F. Liu, P. Heremans, H. Chen, *Mater. Chem. Front.* **2018**, *2*, 121–128.
[17] S. Inayama, Y. Tatewaki, S. Okada, *Polym. J.* **2010**, *42*, 201–207.

Manuscript received: August 5, 2022
Revised manuscript received: October 24, 2022
Accepted manuscript online: November 29, 2022
Version of record online: December 30, 2022